

Video Article

Establishment of a Severe Dry Eye Model Using Complete Dacryoadenectomy in Rabbits

Robert A. Honkanen¹, Liqun Huang^{2,3}, Wei Huang¹, Basil Rigas^{2,4}¹Department of Ophthalmology, Stony Brook University²Department of Medicine, Stony Brook University³Medicon Pharmaceuticals, Inc⁴Department of Preventive Medicine, Stony Brook UniversityCorrespondence to: Robert A. Honkanen at Robert.Honkanen@stonybrookmedicine.eduURL: <https://www.jove.com/video/60126>DOI: [doi:10.3791/60126](https://doi.org/10.3791/60126)

Keywords: Medicine, Issue 155, dry eye, dry eye syndrome, rabbit model, dacryoadenectomy, physiology, ocular drug development, tear breakup time, Schirmer's tear test, tear osmolarity, rose bengal staining

Date Published: 1/8/2020

Citation: Honkanen, R.A., Huang, L., Huang, W., Rigas, B. Establishment of a Severe Dry Eye Model Using Complete Dacryoadenectomy in Rabbits. *J. Vis. Exp.* (155), e60126, doi:10.3791/60126 (2020).

Abstract

Dry eye disease (DED) is a complex disease with multiple etiologies and variable symptoms, having ocular surface inflammation as its key pathophysiologic step. Despite advances in our understanding of DED, significant knowledge gaps remain. Advances are limited in part due to the lack of informative animal models. The authors recently reported on a method of DED induced by injecting all orbital lacrimal gland (LG) tissues with the lectin concanavalin A. Here, we report a novel model of aqueous-deficient DED based on the surgical resection of all orbital LG (dacryoadenectomy) tissues. Both methods use rabbits because of their similarity to human eyes in terms of the size and structure of the ocular surface. One week after removal of the nictitating membrane, the orbital superior LG was surgically removed under anesthesia, followed by removal of the palpebral superior LG, and finally removal of the inferior LG. Dacryoadenectomy induced severe DED, evidenced by a marked reduction in the tear break up time test and the Schirmer's tear test, and significantly increased tear osmolarity and rose bengal staining. Dacryoadenectomy-induced DED lasted at least eight weeks. There were no complications and animals tolerated the procedure well. The technique can be mastered relatively easily by those with adequate surgical experience and appreciation of the relevant rabbit anatomy. Since this model recapitulates the features of human aqueous-deficient DED, it is suitable for studies of ocular surface homeostasis, DED, and candidate therapeutics.

Video Link

The video component of this article can be found at <https://www.jove.com/video/60126/>

Introduction

Tears are required for the protection of the ocular surface and for the maintenance of the optical properties of the cornea. They consist of three layers: an inner mucin coating, a middle aqueous component, and a lipid overlay¹. The mucin layer is produced predominantly in goblet cells of the conjunctiva, the aqueous component predominantly in the lacrimal glands (LGs), and the lipid layer predominantly in the Meibomian glands^{1,2}. The orbital LGs are the main source for the aqueous component of tears and for many of the proteins that protect the surface from bacterial attack³. Ocular surface diseases ensue when the aqueous tear production is decreased below a critical level, depriving the epithelial surfaces of the eye of the aqueous component and crucial tear constituents including growth factors, lysozyme, and lactoferrin. In cases of decreased tear production by the LGs, the conjunctival and corneal tissues undergo adaptations to compensate for the altered environment.

Understanding the contribution of the tear component derived from the orbital LGs and the ocular surface's compensatory mechanisms when this is lacking impacts our appreciation of the physiology and pathophysiology of the anterior segment of the eye and, more broadly, of health and disease in the entire globe. The experimental approach to these issues requires an informative animal model. Consequently, several groups have attempted to develop animal models in which the orbital LGs are removed, thereby facilitating the assessment of the role of tears in ocular health. One such model was recently reported for the mouse⁴. The rabbit offers, however, many distinct advantages over rodent models including similar anatomic and histologic structures of the LG, and perhaps more importantly, similar size and surface area of the cornea and conjunctival tissues when compared to their human counterparts³.

Creation of aqueous deficient dry eye disease (DED) by surgical resection of LG tissue in rabbits is not new. Numerous reports describe resection of LG tissues with varying success reflected in variable changes in tear production measured by the Schirmer's tear test^{5,6,7,8}. A thorough understanding of the relevant anatomy of the rabbit and clarity about the anatomical terminology are very helpful in reproducing this method. A thorough overview of both is provided below.

Anatomy of the lacrimal glands

The rabbit has two orbital LGs: the larger inferior LG (ILG) and the smaller superior LG (SLG; **Figure 1**). The ILG extends along the inferior and posterior aspect of the orbital rim. With the exception of variable size, the anterior portion of the ILG has a fairly uniform bulbous appearance that can be seen as a protuberance in the skin under the globe (**Figure 2**). Because of its characteristic appearance in relation to the rest of the gland, it is referred to as the "head" of the ILG. A portion of the head wraps around and lies on the external surface of the zygomatic bone. This serves as a useful landmark on ultrasound biomicroscopy to guide injections into the ILG. The remainder of the head resides more medially⁹ in the orbit.

Due to the characteristic appearance of the remaining portion of the ILG, which is long and thin, this segment is referred to as the "tail." The tail runs along the inferior orbital rim, from the head of the ILG to the orbital rim where it terminates with variable anatomy at the inferior and posterior orbital rim (**Figure 3A**). The tail lies deep (medial) to the zygomatic bone separated from the orbital contents by a fascial band for most of its course until it reaches the posterior rim of the orbit where it once again extends out over the external surface of the zygomatic bone. The ILG receives its blood supply from branches of the carotid artery.

The SLG has two components analogous to the human. One is the palpebral superior LG (PSLG), which resides in the upper posterior eyelid medial to the tarsal plate. It appears bulbous in nature and has numerous punctate openings that drain aqueous tear fluid that is more easily seen when covered with 2% fluorescein (**Figure 3B**).

The second is the orbital superior LG (OSLG), residing in a medial position in the superior orbit (**Figure 3C**). Due to its position near the midline of the skull, it has been impossible to successfully identify it using external surgical approaches from the temporal or inferior orbit. In fresh necropsy samples or surgical cases, this gland can be prolapsed through the posterior incisure located in the dorsal surface of the skull when gentle medial pressure is applied to the globe. Prolapse of this glandular tissue can be documented with ultrasound biomicroscopy.

The PSLG and OSLG are contiguous structures. The OSLG is a tubuloalveolar structure whose ductal architecture coalesces into the main excretory duct. This duct passes under the supra-orbital ridge and runs in the upper lid tissues terminating in the PSLG. Along the excretory duct, glandular tissue consistent with the original descriptions of Davis has been identified¹⁰ (**Figure 3D**).

A note on terminology

Excellent and comprehensive anatomic descriptions use varying terminology as well. The classic orbital anatomy by Davis defines only an upper and lower LG¹⁰. However, his description of the upper LG clearly details the portions more specifically defined here as the PSLG and OSLG, while his description of the lower LG details the portions defined here as the head and tail of the ILG. A more recent and thorough anatomical atlas¹¹ defines these tissues as the zygomatic gland and the accessory LG. The term "lacrimal gland" is used here to comprise the aforementioned PSLG and OSLG. This terminology is better suited for reproducing this method without undue confusion.

Protocol

All vertebrate animal studies were completed in accordance and compliance with all relevant regulatory and institutional guidelines. All studies were approved by the Institutional Review Board of Stony Brook University and performed in accordance with the Association for Research in Vision and Ophthalmology (ARVO) statement for the use of animals in ophthalmic and vision research.

1. Animals and housing

1. Use New Zealand White (NZW) rabbits weighing 2–3 kg.
2. House rabbits individually in a strictly controlled environment: temperature (65 ± 5 °F), humidity ($45 \pm 5\%$), and lighting (12 h on/off cycle).
NOTE: Due to aggressive behaviors often exhibited between rabbits that are group-housed, keep animals in individual cages to prevent inadvertent ocular injury.
3. Give rabbits unlimited access to standard rabbit chow and water.
4. Provide no other dietary enrichments so as to prevent inadvertent vitamin A supplementation which might affect dry eye.
5. Acclimate rabbits at least two weeks before recording DED parameters.

2. Removal of the nictitating membrane

NOTE: For simplicity, the technique for the right eye is described below. Complete this procedure on the left eye in an identical manner.

1. Remove the nictitating membrane bilaterally during the acclimation period (usually the first week).
2. Place rabbit in an appropriately sized restraining bag.
3. Administer a subcutaneous injection of acepromazine (1 mg/kg) over the shoulders using a 1 cc syringe and 26 G needle to sedate the rabbit. The endpoint for this mild sedation is when the animal maintains a relaxed head position without normal scanning movements and its ears are no longer fully upright.
4. Using a micropipette, apply 25 μ L of preservative-free lidocaine (1%) to the eye. Insert a wire lid speculum between the eyelids.
5. Grasp the nictitating membrane at its apex with 0.3 forceps (or equivalent) and pull it over the corneal surface. Inject 1% lidocaine with 1:100,000 epinephrine into the subconjunctival space of the nictitating membrane using a 26 G needle. Inject approximately 0.3 mL to form a modest-sized bleb over the nictitating membrane. Injection volumes over 1 mL are well within a safe dose range for rabbits (2–4 mg/kg).
6. Remove the wire speculum. Wait approximately 5 min for the lidocaine and epinephrine to take effect. During this time, perform the same procedure in the fellow eye.
7. Replace the wire lid speculum. Grasp and extend the nictitating membrane over the corneal surface using 0.3 forceps. Cut the membrane at its base with tenotomy scissors or equivalent.
NOTE: Bleeding is usually minimal, but keep a high-temperature battery cautery unit nearby and use as needed to minimize bleeding. Direct pressure over the cut base of the nictitating membrane can also be used to stop small bleeding if it occurs.

8. Remove the wire lid speculum. Place topical antibiotic ointment (neomycin, polymyxin, bacitracin, and hydrocortisone) over the corneal surface.
9. Perform an identical procedure to the fellow eye as indicated by the protocol.
10. Place animals back in individual cages and allow to heal for at least one week, or until the conjunctival surface has healed completely from a clinical standpoint, before performing any further assays or interventions.
NOTE: Complete clinical healing is indicated by a lack of any swelling, injection or discharge from the conjunctival surfaces. Animals should keep their eyes open normally, without the presence of protective ptosis.

3. Measurement of dry eye parameters and collection of tear samples

1. Measure the following DED parameters, as appropriate to the experimental protocol: tear osmolarity, tear break-up time, Schirmer's tear test, and rose bengal staining. Perform them as previously described¹², with a team of at least two investigators.
NOTE: A team of at least two investigators allows for the efficient measurement of larger groups of animals (6 or more) around the same clock time thereby preventing possible circadian variation from impacting results.

4. Surgical preparation and anesthesia

1. Lightly sedate animals placed in a restraining bag with subcutaneous acepromazine as above (1 mg/kg).
2. Remove all fur on the face and dorsal surface of the skull to visualize the surgical landmarks.
 1. Trim fur with cutting shears leaving residual fine fur about 1 mm in length (**Figure 4A**, left).
 2. Remove all residual fur using mild depilatory cream following the manufacturer's instructions (**Figure 4A**, right).
3. Mark surgical incision sites with a surgical pen.
 1. Identify the incision site over the posterior incisure by applying medial pressure to the globe causing a small bulge to develop in the skin over the posterior incisure from prolapse of the OSLG.
 2. Make a linear 2 cm mark in the anterior/posterior direction on the skin over the dorsal surface of the skull directly over this site with a surgical marking pen.
 3. When planning the incision for removal of the ILG, mark a long, curvilinear line around the eye (1 cm from the inferior and temporal lid margin) extending from the posterior (temporal) orbit to the anterior (medial) canthus. Make the marking extend along the posterior orbit to the level of the medial canthus or just superior to this (**Figure 4B**). In some dissections, the incisions to remove the OSLG and the ILG will be connected.
NOTE: When performing bilateral surgery, mark both orbits at this time.
4. Trim a patch of fur 2 to 3 cm wide with shears over the lateral surface of each thigh to allow placement of a monopolar cautery plate.
 1. Apply ultrasound gel to ensure good electrical contact with the monopolar cautery plate.
5. Place a 25 G intravenous (IV) catheter in one of the marginal veins of the ear to administer medications or fluids if needed.
6. Give subcutaneous xylazine (1 mg/kg) and IV ketamine (15 mg/kg) for the initial induction of anesthesia (through the IV access).
NOTE: If the rabbit is sedated beforehand with acepromazine sufficient to retain the endpoint described in step 2.3, use gas mask sedation with isoflurane as an alternative.
7. Place a laryngeal mask airway held in place using an elastic band or string to secure and maintain the airway.
 1. Connect the mask to the anesthesia machine with oxygen flow set at 1 L/min.
 2. Set the isoflurane at 5% initially and then reduce as tolerated based on the level of animal sedation.
 3. Maintain isoflurane at or above 2% until final wound closure.
NOTE: Assess the level of sedation by monitoring for respiratory rate and movements in response to surgical or painful stimuli. Increase the depth of anesthesia if respiratory rate increases above 10 breaths per minute, if the rabbit begins to chew on the airway maintainer, or if any movements in response to painful stimuli are observed.
8. Monitor pulse oximetry, capnography, blood pressure, rectal body temperature and heart rate using a multi-parameter monitoring device or other appropriate devices.
 1. Monitor vitals continuously during the procedure and record every 10 to 15 min.
9. Position the rabbit on the operating room (OR) table over a heating pad to prevent hypothermia. Tilt the table in a reverse Trendelenburg position at approximately 30° to minimize bleeding.
10. Prepare the surgical area with a povidone-iodine solution diluted to half-strength with sterile water and drape so as to maintain a sterile field.

5. Complete surgical dacryoadenectomy

NOTE: The complete surgical dacryoadenectomy, as described herein, was done using 0.3 tissue forceps, tenotomy scissors, non-toothed tissue forceps, and scissors. These instruments can be interchanged with similar instruments that perform the same function based on surgeon preference.

1. Remove the OSLG first.
 1. Infiltrate the incision sites (surgical marking pen lines and upper posterior lid) with a 50:50 mixture of 2% lidocaine with 1:100,000 epinephrine and 0.5% bupivacaine using a 5 cc syringe with a 30 G needle (**Figure 5A**).
NOTE: Syringe and needle size are not critical.
 2. Use a Colorado needle connected to an electrosurgical unit to make the skin incisions along the surgical markings. Settings can vary based on clinical response and typically are between 10 to 15 units for both cut and coagulation (**Figure 5B**).
 3. Apply opposing tension across the skin incision to separate the tissues and expose the underlying frontoscutularis muscle fibers.

4. Apply medial pressure on the globe to aid visualization of the OSLG, seen as bulging tissue located just medial or deep to the frontoscutularis muscle fibers. If necessary, move these muscle fibers to the side in order to expose the underlying incisure.
 5. With toothed forceps (0.3) and capsulotomy scissors, gently retract and cut the fibrous capsule overlying the OSLG. The OSLG typically has a pale tan color (**Figure 5C**).
 6. Using toothed or non-toothed forceps, grasp the OSLG gland tissue and gently pull it out through the superior incisure using a "hand over hand" technique. Cut small, fibrous bands using capsulotomy scissors to free the gland from its position in the orbit (**Figure 5D**). NOTE: As the OSLG gland tissue is removed, it will begin to coalesce into a large tube-like structure (main excretory duct).
 7. When the gland has been removed as completely as possible, use generous cautery with the Colorado needle to create tissue char, truncating the gland within the incisure as deeply as possible. This will later serve as a confirmatory landmark during removal of the PSLG.
2. Remove the PSLG.
 1. Evert the upper eyelid using a cotton-tipped applicator. The bulbous end of the PSLG is usually easily visible. NOTE: In some anatomic dissections, it may be possible to visualize the main excretory duct as a pale linear structure about 1 or 2 mm wide.
 2. Engage the PSLG with toothed forceps (0.3) and retract it from the eyelid surface while using capsulotomy scissors to cut around its base separating it from the underlying tarsus (**Figure 6A**).
 3. Control moderate bleeding with the monopolar cautery.
 4. Apply continuous traction on the separated tissue to maintain a tissue plane for dissection. This will allow the main excretory duct of the SLG to be removed as well (**Figure 6B**). NOTE: As the dissection is carried out, it will typically advance to the superior orbital rim where it is possible to see the cautery marks left behind from removal of the more superior and medially located OSLG.
 3. Resect the ILG.
 1. Allow at least 5 min for the local anesthetic to take effect.
 2. Incise the skin, the depressor muscle of the inferior palpebra, the zygomaticolabial part of the zygomatic muscle, and orbicularis muscle with the Colorado microdissection needle and separate as for the OSLG in section 5.1.
 3. Maintain hemostasis with the monopolar cautery.
 4. As the incision is carried deeper through the skin marking, look for the sheen of a fascial plane over the zygomatic bone or superficial part of the masseter muscle. At this point, maintain the tissue plane and carry it superiorly toward the orbital rim using the Colorado needle for cutting (**Figure 7A**). NOTE: For the purpose of identifying the ILG, it is easiest to perform this part of the dissection over the head of the ILG which is typically inferior to the anterior limbus of the eye.
 5. After identifying and incising the capsule surrounding the ILG, identify the tan tissue of the ILG. Only the anterior portion of the ILG head will be visible (**Figure 7B**). However, the head can be followed medially as it passes beneath the zygomatic arch and transitions into the tail (**Figure 7C**).
 6. Use tenotomy scissors to cut the orbital septum along the inferior rim exposing the more posterior portion of the ILG tail. Once the tissue plane is identified, extend the dissection posteriorly along the entire incision line (**Figure 7D**). NOTE: The duct of the ILG passes through the lower fibrous connective tissues to enter the inferior conjunctival space in the temporal aspect of the lid. At the posterior rim, the tail of the ILG can have varying anatomic configurations. Sometimes it terminates inferior to the posterior (lateral) canthus, while in other dissections it extends more superiorly around the temporal orbit.
 7. Use extreme care to prevent inadvertent damage to the blood supply, which the ILG receives from branches of the carotid artery. The blood supply can be seen during this part of the dissection (**Figure 7E**).
 8. In cases where the tail terminates under the posterior (lateral) canthus, it may be necessary to bisect the temporal portion of the frontoscutular muscle to expose the tail of the ILG, which lies along the zygomatic bone.
 9. After the entire ILG has been isolated and exposed, remove it. Due to its large size, it is often preferable to cut the gland in half with scissors and remove the head separately from the tail.
 10. Proceed very cautiously when removing the head of the ILG as it lies immediately adjacent to a large venous sinus in the orbit. Although bleeding from this structure during surgical resections has not occurred, have ample hemostatic aids present to mitigate this risk.
 11. After removal of all gland tissue, close the deep connective tissue plane with multiple interrupted 5-0 ethylene terephthalate sutures. Close the superficial muscles and skin with a running 6-0 polyglactin 910 suture (**Figure 7F**) using 0.3 tissue forceps and a needle driver.

6. Postprocedural care

1. Undrape the animals and cleanse the surgical sites with sterile water.
2. Apply topical ophthalmic antibiotic and steroid ointment (neomycin, polymyxin, bacitracin, and hydrocortisone) to the incisions. Continue this application twice a day for 2 days.
3. Give a subcutaneous injection of 20 mL normal saline over the shoulder blades using a 26 G needle.
4. Give subcutaneous buprenorphine 0.01 mg/kg or ketoprofen 3 mg/kg for pain control using a 1 cc syringe and 30 G needle. NOTE: Animals should return to their normal dietary intake and activities within 1–2 days. Rabbits should be evaluated at least weekly for clinical signs of infection as evidenced by progressive swelling, pain, erythema, calor or purulent discharge over the incision sites. Animals must also be observed to make sure they do not begin to scratch the incision sites/suture lines. Trimming all claws prior to dacryoadenectomy may be helpful in this regard. If scratching the incision lines is observed, standard protective collars may be used to prevent self-injury.
5. Reverse the anesthesia.
 1. Remove the airway maintainer after the animal responds to stimuli and begins to show spontaneous chewing but before the airway maintainer can be damaged.

2. Monitor animals for approximately 1–2 h or until they have completely recovered from anesthesia as evidenced by spontaneous movement in their cages.
 3. Assess animals for pain and treat appropriately.
6. Allow animals to recover for at least 1 week following surgery before making any clinical measures of DED.

Representative Results

The complete dacryoadenectomy method described here was performed on 8 animals. It requires a moderate degree of surgical skill. Surgical time averaged about 2.2 h for bilateral surgery, excluding the removal of the nictitating membrane, which was done separately and required <10 minutes. There were no fatalities or intraoperative complications and no rabbit required any hemostatic aid other than modest cautery.

Our surgical approach successfully induced dry eye in all eyes. This was confirmed by a panel of clinical and laboratory markers of DED (Table 1). During the 8 weeks of observation, the mean TBUT was suppressed by more than 75% of preoperative levels ($p < 0.0001$ for all time points). Similarly, the Schirmer's tear test decreased by approximately 50%, remaining so for the 8 weeks of observation; it showed no trend for recovery during the follow up period. Postoperatively, tear osmolality showed a 10% increase consistent with DED, sustained for at least 8 weeks postoperatively. Rose bengal staining of the cornea also increased and did not show signs of recovery during the 8 weeks of follow-up (Figure 8). All eyes undergoing complete dacryoadenectomy showed marked reduction in goblet cell numbers and epithelial changes consistent with dry eye (conjunctival impression cytology).

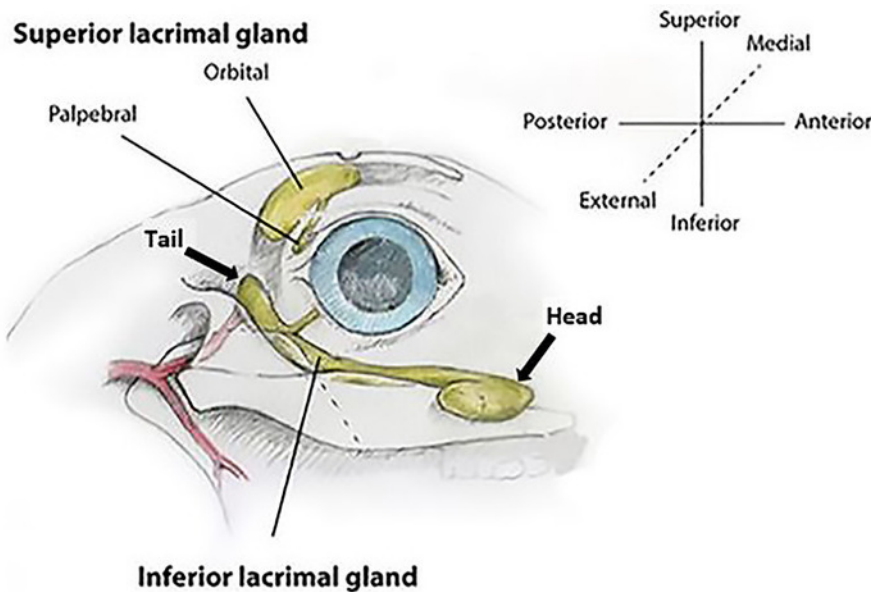


Figure 1: Rabbit lacrimal gland anatomy (right eye). The orbital superior lacrimal gland (OSLG) is comprised of a larger orbital part and smaller palpebral component. The larger inferior lacrimal gland (ILG) is comprised of the anterior/head and posterior/tail portions. Coordinate axes show the terminology used for all descriptions of orientation used within the text. [Please click here to view a larger version of this figure.](#)

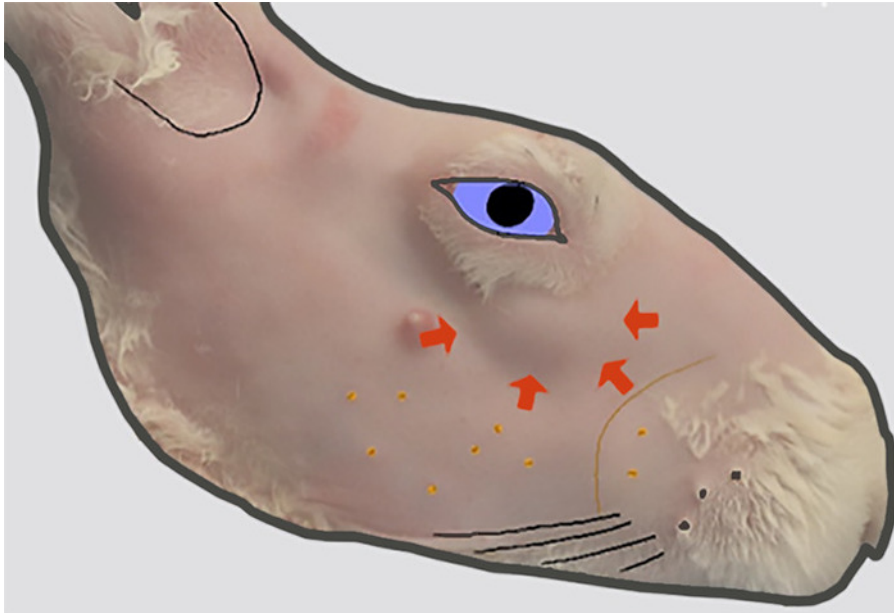


Figure 2: Location of the head of the ILG. The lateral view of the right face after removal of fur. A bulge in the skin contour (indicated by thick arrows) inferior to the anterior orbit indicates the location of the head of the ILG that lies on the external surface of the zygomatic bone at this location. [Please click here to view a larger version of this figure.](#)

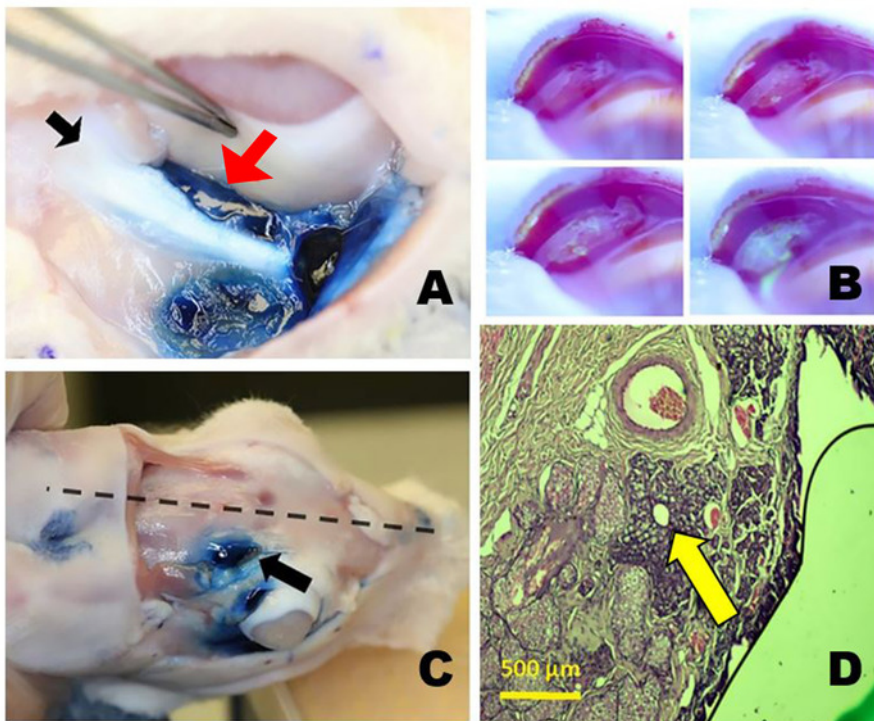


Figure 3: The orbital lacrimal glands. (A) The right inferior lacrimal gland (ILG) after staining with Evans blue dye showing the close proximity of the tail of the ILG (red arrow) just medial to the zygomatic bone (black arrow) and inferior to the globe. (B) Tear production from the palpebral superior lacrimal gland (PSLG). Time-lapse photos taken after topical application of 2% fluorescein. Aqueous fluid emanating from the PSLG dilutes the initially dark blue or black fluorescein dye turning it bright yellow green (similar to Seidel testing). (C) Position of orbital SLG (OSLG) in the rabbit skull, lying close to the midline of the skull (dotted line) within the posterior incisure (arrow). Evans blue dye was injected into the OSLG and palpebral superior lacrimal gland. (D) Histology section through the main excretory duct of the OSLG surrounded by a small amount of glandular tissue (arrow) is seen in this histopathologic cross-section stained with hematoxylin and eosin dyes taken through the posterior (temporal) aspect of the upper right eyelid. [Please click here to view a larger version of this figure.](#)

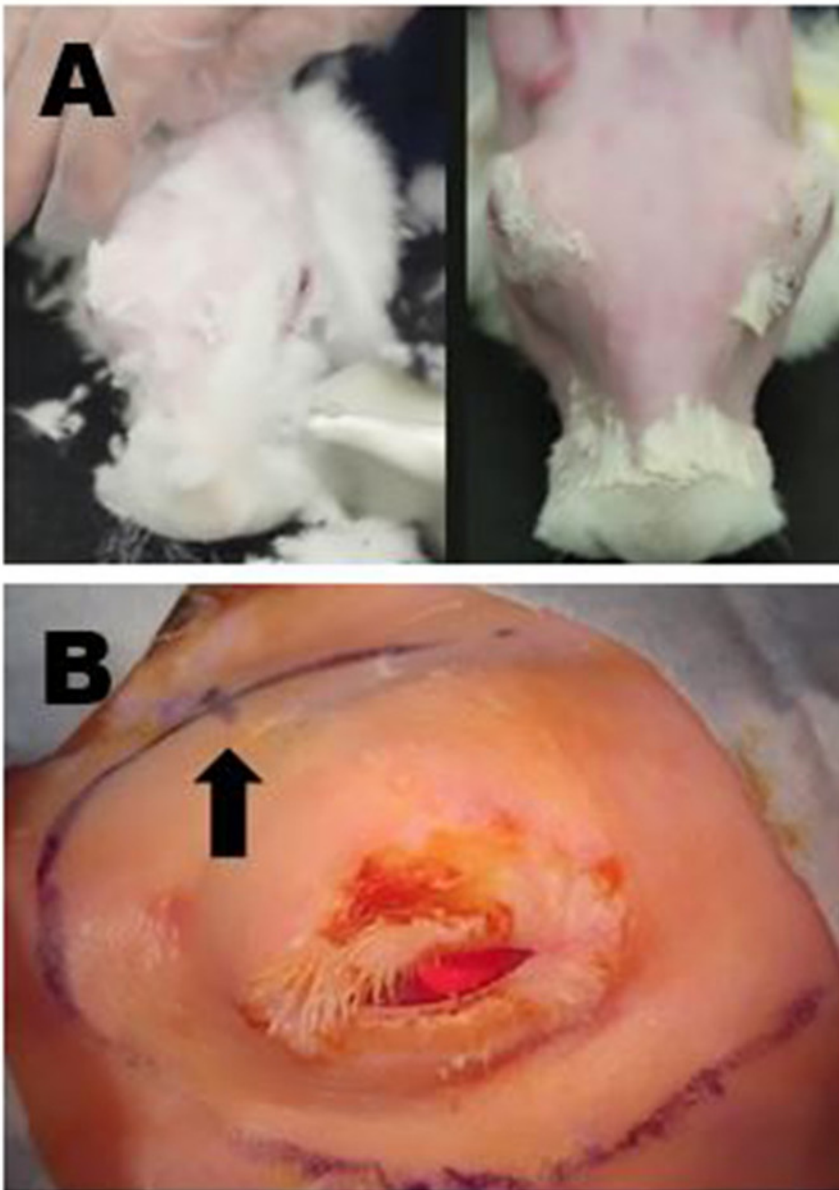


Figure 4: Surgical site preparation. (A) Upper left panel: Removal of long fur with shears. All residual fine fur is subsequently removed with a mild depilatory cream. Upper right panel: Final appearance following complete fur removal that allows for surgical marking and high-quality ultrasound of the ILG to be performed. (B) Appropriate surgical markings of the right periorbital region are shown; in this example, the incisions to remove the OSLG and ILG have been connected to create one long curvilinear incision. The location of the posterior incision is indicated by a small hash mark on the curvilinear incision site marking (arrow). [Please click here to view a larger version of this figure.](#)

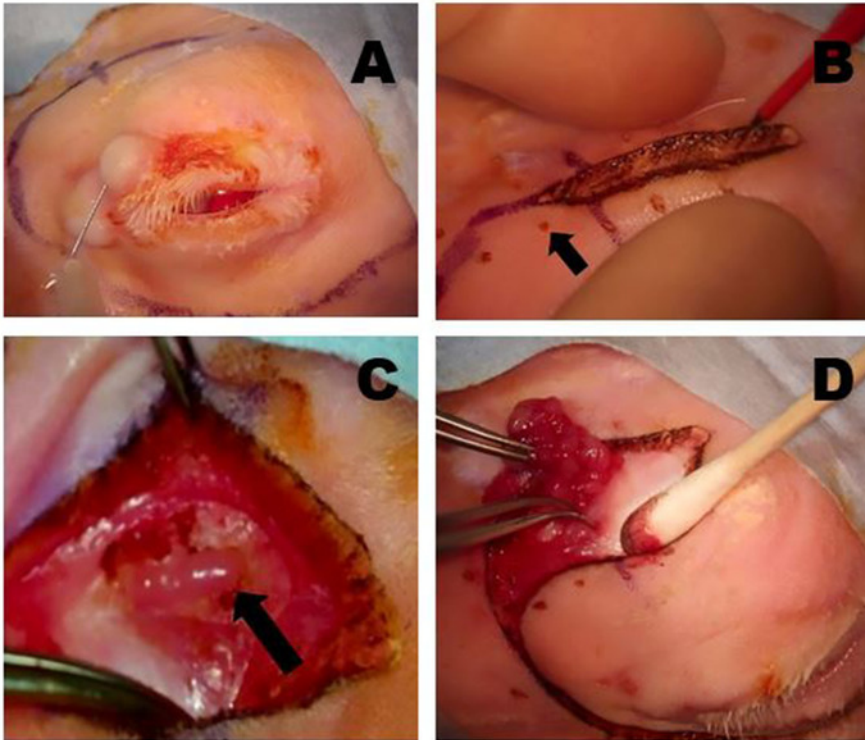


Figure 5: Removal of the OSLG. (A) Surgical sites are infiltrated with anesthetic using a 50:50 combination of 2% lidocaine with 1:100,000 epinephrine and 0.5% bupivacaine, which is injected into the upper lid and along the incision lines to minimize discomfort during the procedure. (B) A Colorado microdissection needle is used to incise the skin and superficial muscle layers along the pre-marked surgical incision sites. Gentle traction across the wound is applied to help create the dissection plane. The small pinpoint burns (arrow) were made with the Colorado needle at equidistant points along the incision line to help optimally realign the tissues during wound closure. (C) The OSLG is exposed after tissues overlying the posterior incisure have been mobilized (arrow). The capsule of the gland has been incised. The OSLG can be prolapsed by applying medial pressure to the globe facilitating its removal. (D) Forceps are used to engage the OSLG and gently remove it from its deeper position within the orbit through the posterior incisure. [Please click here to view a larger version of this figure.](#)

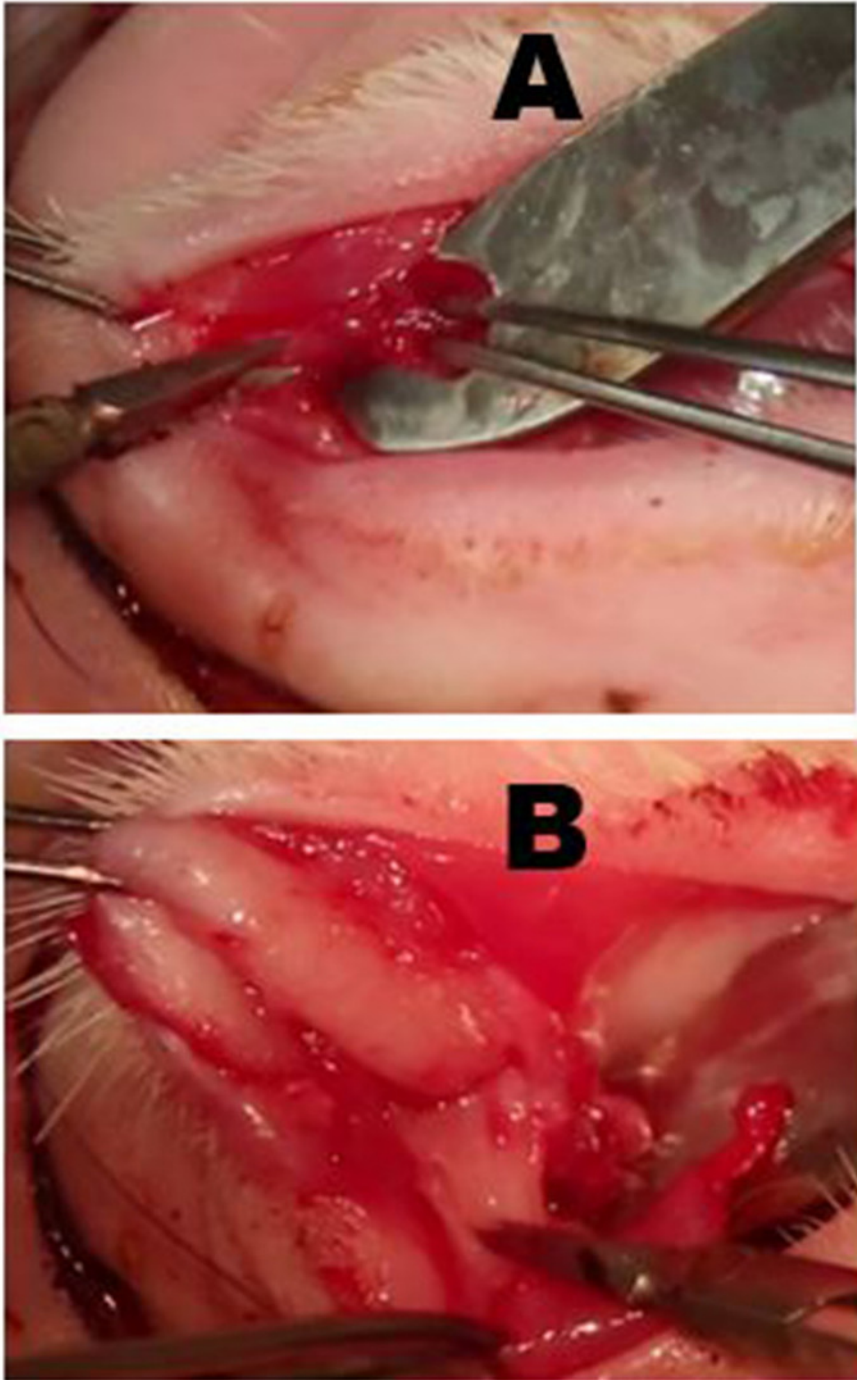


Figure 6: Removal of the palpebral superior lacrimal gland (PSLG) and excretory duct. (A) Following eversion of the upper eyelid, the bulbous portion of the PSLG is engaged with forceps and dissected off the tarsus using scissors. Traction applied to the PSLG with forceps is critical to maintaining the surgical plane. (B) The dissection of the PSLG and the main lacrimal duct is carried superiorly toward the orbital rim using sharp dissection and continuous traction on the gland and duct tissues to maintain the appropriate surgical plane. The dissection should proceed to the point where the OSLG was removed. [Please click here to view a larger version of this figure.](#)

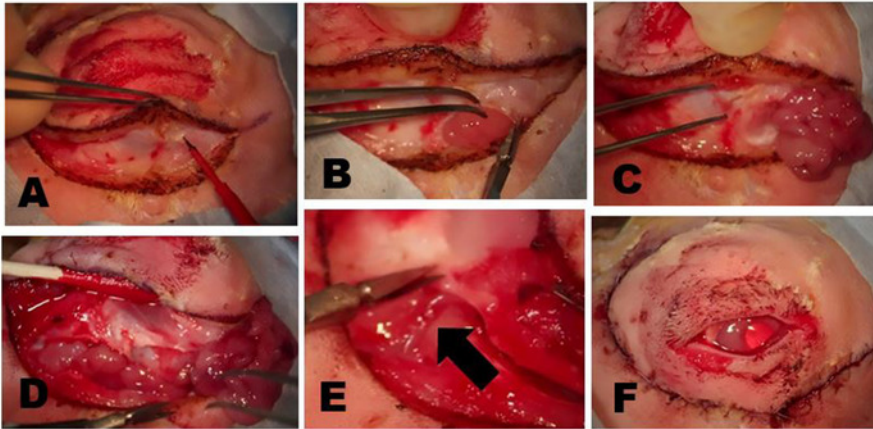


Figure 7: Removal of the ILG. (A) The skin and superficial muscle are incised until the fascial plane overlying the zygomatic bone or superficial part of the masseter muscle is reached. The head of the ILG usually is clearly evident as a small bulge located under the anterior limbus. (B) The fibrous capsule of the ILG is incised with scissors exposing the ILG. Once the capsule is incised, the deeper portions of the gland can be easily removed. (C) The most external portion of the ILG head that lies on the zygomatic bone has been exposed and reflected anteriorly showing the underlying zygomatic bone. (D) Incision of the orbital septum along the inferior rim exposes the tail of the ILG. (E) A branch of the external carotid artery feeds the tail of the ILG (arrow). (F) Appearance following the closure of skin incisions after complete dacryoadenectomy. [Please click here to view a larger version of this figure.](#)

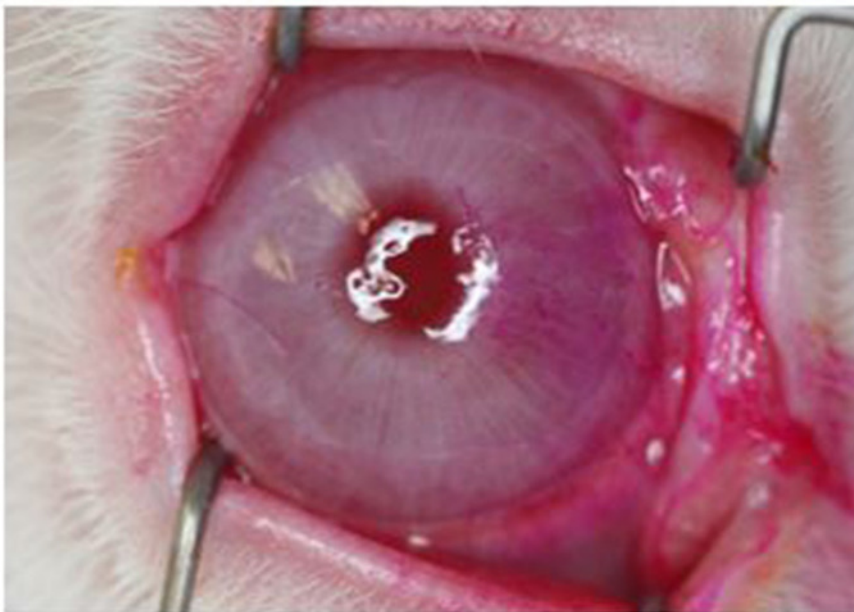


Figure 8: Rose Bengal staining of the corneal surface. External photograph showing prominent staining, most notable on the nasal quadrant. All eyes undergoing complete dacryoadenectomy developed similar changes that were evident by 1 week after surgery and persisted for at least 6 weeks. Of note, the light reflex from the ring flash shows distortion from a dry ocular surface demonstrating how dry eye can adversely impact vision. [Please click here to view a larger version of this figure.](#)

Dacryoadenectomy		
<i>mean ± SEM; n = 16 eyes</i>		
	Baseline	Week 2
Tear break-up time, s	60.0 ± 0.0	4.5 ± 1.2 p < 0.0001
Tear osmolarity, mOsm	291.2 ± 3.7	315.3 ± 5.5 p = 0.001
Schirmer tear test, mm	18.3 ± 1.3	10.5 ± 1.6 p = 0.0006
Rose bengal, modified NEI score	0.0 ± 0.0	4.28 ± 0.6 p < 0.0001

Operated vs. baseline: *Dacryoadenectomy*: TBUT, p < 0.0001; tear osmolarity, p < 0.001; Schirmer tear test, p < 0.0006; and rose bengal.

Table 1: Dry eye parameters on postoperative week 2.

Discussion

DED is classified into two major groups based on the effect on tear film stability: aqueous deficient (decreased production of the aqueous component of the tear film; ~20% of DED) and evaporative (increased evaporation of the tear film; ~50% of DED). About 30% of DED patients show evidence of both (mixed DED). Inflammation is the core mechanism of DED to which its diverse etiologies converge^{13,14}. Our method models aqueous-deficient DED.

As previously mentioned, important first steps in reproducing our method are an appreciation of the fine points of the anatomy of the orbital lacrimal glands (LGs) of the rabbit and avoiding confusion by varied and sometimes conflicting anatomical terminology. The anatomical atlas by Popesko et al.¹¹ is extremely thorough. For those less comfortable with the anatomy of the rabbit, dissection of necropsy specimens provides easy familiarity with these structures and aids their surgical removal in living specimens.

Critical advice on animal housing and acclimation has been given in our companion publication¹². The same article also presents useful comments for assaying the parameters of DED used in both methods.

In contrast to the previous method¹², this one requires a higher level of surgical skill because of the extent and more invasive nature of the techniques needed to remove the LGs. The greatest risk during these resections is catastrophic bleeding caused by injuring major vessels that are in close proximity to the LGs such as branches of the carotid artery. This is avoided by adequately visualizing each LG and its margins within the surgical field. Finally, overzealous removal of the nictitating membrane could lead to the prolapse of the Harderian gland, which can disrupt tear film assessment.

Care should be taken to minimize the amount of conjunctival disruption with the removal of the PSLG, a novel aspect of our method that improves reproducibility and enhances the severity of DED. It is surprisingly easy to establish the dissection plane and carry it back to the superior orbital ridge as long as traction is applied to the tissues. It is reassuring to be able to see the cautery marks from the truncation of the OSLG; they confirm the complete removal of the main excretory duct of the gland.

Removal of the ILG in its entirety presents challenges as well. Isolate the head of the gland first, as this is the easiest part to visualize. The entire head of the gland tissue separates easily from the surrounding tissues; however, some care must be used to prevent damage to the large venous sinus, which lies medial to the head of the ILG. The tail of the ILG can then be followed back as it passes under the zygomatic bone. The majority of the tail is easy to isolate. However, the most posterior aspect of the tail can prove more challenging because of variable anatomy and its proximity to a medium-sized branch of the carotid. Careful dissection should allow all margins of the ILG to be seen clearly, facilitating its complete removal. The investigator should be prepared to carry the dissection more superiorly in cases where the tail of the gland ends under the lateral canthus, as explained in the earlier discussion of the anatomy of the lacrimal glands. Of note, the authors have never been able to identify any portion of the OSLG when dissecting the ILG through a curvilinear incision along the temporal and inferior globe. Although this may be technically possible, that surgical approach carries too high a risk for serious bleeding. Approaching the OSLG through the posterior incisure proves far safer.

The excretory duct of the ILG can be seen penetrating through the inferior fascial plane as it passes into the lower conjunctival fornix. Occasionally, small lobules of glandular-appearing tissue are seen here as well and can be carefully removed.

It is very helpful to maintain the order of LG resection as presented here. If the ILG is removed first, the isolation of the OSLG becomes technically far more difficult. The main reason is that, after removal of the ILG, the OSLG cannot be easily prolapsed and thereby identified.

A significant advantage of our model is that it can be "modular." In other words, the degree of DED induced by dacryoadenectomy can be calibrated to serve experimental needs. For example, resection of all LGs would cause maximal DED, but resection of only the SLG would cause the mildest form of DED and resection of only the ILG would generate disease of intermediate severity.

Our approach, which recapitulates the distinct pathophysiological event of reduced tear production offers additional advantages compared to already reported methods. Briefly, no other surgical model eliminated tear production by all orbital LGs^{5,6,7,15,16}, including parasympathetic

denervation of the LGs¹⁷, and pharmacological suppression of tear production^{18,19}, with the latter two having their off-target effects as significant confounders. Finally, this model minimizes the main investigator-dependent bias, namely the incomplete resection of the LGs, since the surgical technique affords their complete visualization; this is aided by the fact that no hemostasis, other than cautery, is required.

The investigator should be cognizant that complete resection of all orbital LGs does not generate complete absence of tears, and, for example, Schirmer's tear test values approaching zero should not be expected. This is due to the fact that there are always other sources of tear fluid such as the accessory LGs of Wolfring and Krause and plasma leakage from conjunctival vessels^{20,21,22}. From an experimental standpoint, this should be viewed as a positive aspect of the method as it maintains the ocular surface; complete xerophthalmia would totally destroy the cornea negating the usefulness of the model. Additionally, in its current embodiment, this model offers an excellent opportunity to study such compensatory mechanisms and fluid transport across these smaller compartments.

In conclusion, presented here are the specifics of a novel and versatile method of inducing aqueous-deficient DED that lends itself to the study of tear physiology, the pathogenesis of DED and the study of therapeutic agents being developed for this indication.

Disclosures

The authors declare no competing interests except for BR who has an equity position in Medicon Pharmaceuticals, Inc. and Apis Therapeutics, LLC; and LH, an employee of Medicon Pharmaceuticals, Inc. with an equity position in Apis Therapeutics, LLC.

Acknowledgments

We acknowledge the financial support from a Targeted Research Opportunities grant from the Stony Brook University School of Medicine and a research grant from Medicon Pharmaceuticals, Inc., Setauket, NY. We thank Michele McTernan for editorial support.

References

- Gillan, W. D. H. Tear biochemistry: A review. *South African Optometrist*. **69** (2), 100-106 (2010).
- Conrady, C. D., Joos, Z. P., Patel, B. C. Review: The Lacrimal Gland and Its Role in Dry Eye. *Journal of Ophthalmology*. **2016**, 7542929 (2016).
- Schechter, J. E., Warren, D. W., Mircheff, A. K. A lacrimal gland is a lacrimal gland, but rodents' and rabbits' are not human. *Ocular Surface*. **8** (3), 111-134 (2010).
- Shinomiya, K., Ueta, M., Kinoshita, S. A new dry eye mouse model produced by exorbital and intraorbital lacrimal gland excision. *Scientific Reports*. **8** (1), 1483 (2018).
- Bhattacharya, D. *et al.* Tear Production After Bilateral Main Lacrimal Gland Resection in Rabbits. *Investigative Ophthalmology and Visual Science*. **56** (13), 7774-7783 (2015).
- Chen, Z. Y., Liang, Q. F., Yu, G. Y. Establishment of a rabbit model for keratoconjunctivitis sicca. *Cornea*. **30** (9), 1024-1029 (2011).
- Li, N. *et al.* Establishment of the mild, moderate and severe dry eye models using three methods in rabbits. *BioMed Central Ophthalmology*. **13** 50 (2013).
- Honkanen, R. *et al.* A New Rabbit Model of Chronic Dry Eye Disease Induced by Complete Surgical Dacryoadenectomy. *Current Eye Research*. 1-10 (2019).
- Nisha, S., Deepak, K. An Insight Into Ophthalmic Drug Delivery System. *International Journal of Pharmaceutical Studies and Research*. **3** (2), 9-13 (2012).
- Davis, F. A. The Anatomy and Histology of the Eye and Orbit of the Rabbit. *Transactions of the American Ophthalmological Society*. **27**, 400.2-441 (1929).
- Popesko, P., Rajitova, V., Horak, J. *A Colour Atlas of the Anatomy of Small Laboratory Animals*. Vol. 1, Rabbit - Guinea Pig. Saunders. Philadelphia, PA (1992).
- Honkanen, R. A., Huang, L., Rigas, B. A rabbit model of aqueous-deficient dry eye disease induced by concanavalin A injection into the lacrimal glands: Application to drug efficacy studies. *Journal of Visualized Experiments*. e59631 (2019).
- Wei, Y., Asbell, P. A. The core mechanism of dry eye disease is inflammation. *Eye & Contact Lens*. **40** (4), 248-256 (2014).
- Pflugfelder, S. C., de Paiva, C. S. The Pathophysiology of Dry Eye Disease: What We Know and Future Directions for Research. *Ophthalmology*. **124** (11S), S4-S13 (2017).
- Gilbard, J. P., Rossi, S. R., Gray, K. L. A new rabbit model for keratoconjunctivitis sicca. *Investigative Ophthalmology and Visual Science*. **28** (2), 225-228 (1987).
- Odaka, A. *et al.* Efficacy of retinol palmitate eye drops for dry eye in rabbits with lacrimal gland resection. *Clinical Ophthalmology*. **6**, 1585-1593 (2012).
- Toshida, H., Nguyen, D. H., Beuerman, R. W., Murakami, A. Evaluation of novel dry eye model: preganglionic parasympathetic denervation in rabbit. *Investigative Ophthalmology and Visual Science*. **48** (10), 4468-4475 (2007).
- Burgalassi, S., Panichi, L., Chetoni, P., Saettone, M. F., Boldrini, E. Development of a simple dry eye model in the albino rabbit and evaluation of some tear substitutes. *Ophthalmic Research*. **31** (3), 229-235 (1999).
- Xiong, C. *et al.* A rabbit dry eye model induced by topical medication of a preservative benzalkonium chloride. *Investigative Ophthalmology and Visual Science*. **49** (5), 1850-1856 (2008).
- Shiue, M. H. *et al.* Pharmacological modulation of fluid secretion in the pigmented rabbit conjunctiva. *Life Science*. **66** (7), PL105-111 (2000).
- Li, Y. *et al.* Rabbit conjunctival epithelium transports fluid, and P2Y2(2) receptor agonists stimulate Cl(-) and fluid secretion. *American Journal of Physiology: Cell Physiology*. **281** (2), C595-602 (2001).
- Dartt, D. A. Regulation of mucin and fluid secretion by conjunctival epithelial cells. *Progress in Retinal and Eye Research*. **21** (6), 555-576 (2002).